Interpreting fault-related gas leakage

Mohammed Alarfaj and Don C. Lawton

ABSTRACT

Faults in extensional regimes can act as gas migration pathways when in contact with a hydrocarbon source. The gas presence associated with the leaking faults may be detected in seismic surveys. The seismic response of waves traveling through low velocity intervals within the leakage zone shows incoherent reflections characterized by vertical chaotic patterns. Seismic attributes such as semblance and curvature assist in detecting these unique characteristics. Multi-attributes could be used together to highlight the locations of the leaking faults.

INTRODUCTION

The work shown in this report was initiated by a study conducted in an active tectonic zone to map the major structure and faults from a 3D seismic survey. The data used for this study was from Te Kiri 3D survey located on the southwest Taranaki Peninsula in New Zealand (Figure 1a). The survey was acquired after predictions of commercial prospectivity in the area after drilling the exploration well, Te Kiri-1 (Todd Energy, 2006). This well showed indications of the presence of oil and gas in the Miocene- and Eocene-aged reservoir sequences.

Mapping the major faults in the survey lead to observations of the presence of gas leakage associated with these faults. The interpretation of gas leakage provides important information about hydrocarbon history, migration paths, integrity of sealing faults, ranking prospects, detecting spill points, identifying drilling hazard and overpressure zones (Aminzadeh et. al., 2002). This report highlights observations and interpretations of fault-related gas leakage in Te kiri 3D. The regional geology explains the presence of the gas leakage which has characteristics detectable by seismic attributes.

GEOLOGICAL BACKGROUND

Taranaki Basin has gone under different deformation stages which affected the distribution of hydrocarbons in the basin (Figure 2). Studies of this basin reveal three main phases of deformations (King and Thrasher, 1996). The first phase started during the break up of Gondwana in the late Cretaceous to Paleogene extension. Normal faults were created, defining the structure of the basement and forming grabens hosting most of source rock deposits. The second phase of deformation occurred due to contraction in the late Eocene to Miocene, resulting in folding and inversion of older faults. Structural closures and migration pathways were formed during this phase. The third deformation phase was extension in the Pliocene to Holocene resulting in northeast-striking normal faults. Some of the late-stage faults cut through the seal of pre-existing closures, causing leakages of trapped hydrocarbons.

Sediments in Taranaki basin are of late Cretaceous age and younger (Figure 1b). Most discovered hydrocarbons are trapped in the top of anticlines and in the footwalls of normal faults (Ilg et al., 2012)

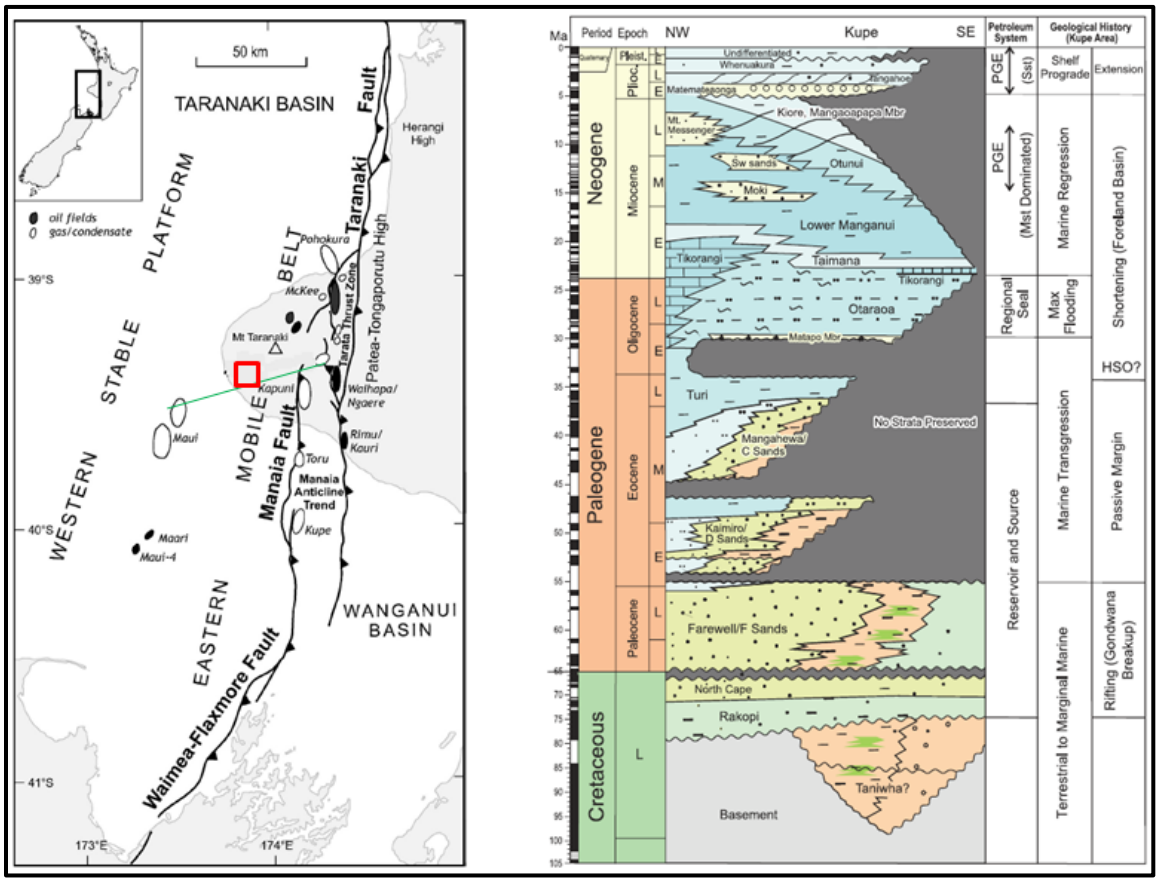

Figure 1: (a) Te Kiri 3D survey area in red box, cross-section by Fig.2 by green, (b) Stratigraphic column (Ilg et al., 2012)

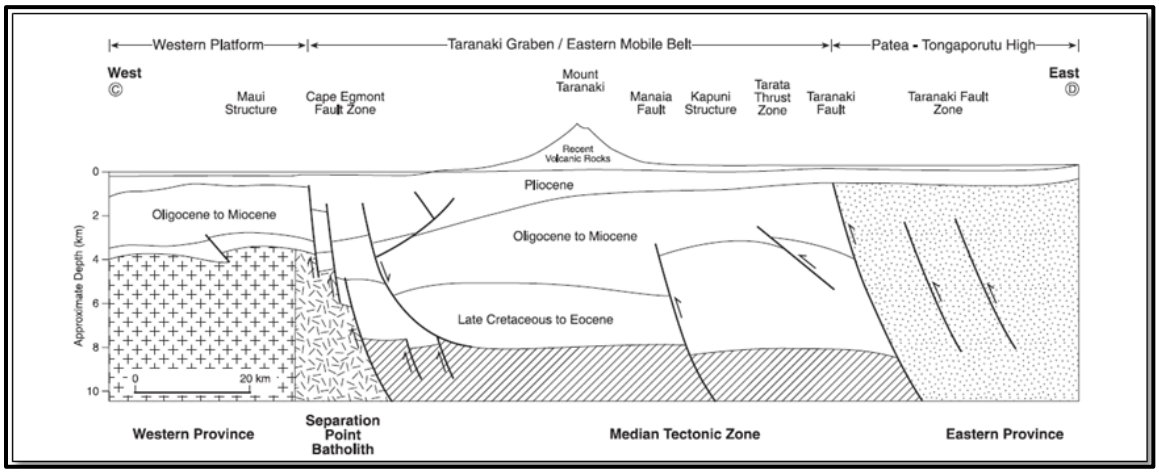

Figure 2: Cross-section showing the general structure (after R. J. Muir et al., 2000)

GAS LEAKAGE CHARACTERISTICS

The presence of gas leaking from faults or fractures might be detected by the acoustic seismic response. This response can be interpreted qualitatively in 3D seismic volumes in conventional slices and vertical sections (Løseth et al., 2009). Gas Leakage shows acoustic changes appearing as vertical chaotic disturbances with amplitude anomalies associated with irregular distribution of low-velocity zones. This vertical incoherence is a result of scattering, attenuation, and decrease in compressional velocity of waves passing through gas saturated pores (Anderson and Hampton, 1980). The gas leakage often appears in vertical sections as cone-shaped distortion when associated with faults (Ilg et al., 2012). When fluids move upward through permeable faults, gas molecules typically get released due the drop in pressure (Bjørkum et. al, 1998). When gas replaces formation water, the contrast of impedance increases and causes the amplitude variations to show as dim and bright spots. This phenomenon is well-illustrated in time-lapse studies (Lawton et. al., 2006 and Alshuhail and Lawton, 2007). The decrease of P-wave velocity due to gas presence explains the seismic push down often observed within the leakage zone. The velocity drop is due to the changes in density and bulk modulus caused by the gas presence. Mathematically, this is explained in a simplified medium (i.e. elastic, homogeneous, and isotropic) by (Mavko et al., 2003):

$$Vp = \sqrt{\frac{K + \left(\frac{4}{3}\right)\mu}{\rho}}$$

where K is bulk modulus, μ is shear modulus, and ρ is density. Pore pressure and temperature affect the bulk modulus and density values. However, even at increased pore pressure values, bulk modulus remains the main parameter affecting the change in P-wave velocity due to the high compressibility of gas which reduces bulk modulus K (Anderson and Hampton, 1980). This explains the drop in compressional velocity due to the gas presence, regardless of the decrease in density.

S-wave velocity, on the other hand, is not as affected by compressibility of gas. Mathematically described in a simplified medium:

$$Vs = \sqrt{\frac{\mu}{\rho}}$$

The P-wave sensitivity and S-wave insensitivity to gas presence explain the advantage of converted-wave imaging through gas-charged sediments as explained by Stewart et al. (2003).

SEISMIC ATTRIBUTES

Seismic attributes are information extracted from seismic data. Attributes could be directly measured or could be interpreted by logic and experience. By understanding the characteristic response of waves passing through gas, leaky faults could be predicted by the output of these measurements. The most effective attributes are the ones that amplify the contrast between the gas response and non-gas responses. Several useful attributes applied in this study were categorized by Taner (2001) as geometrical attributes. These attributes scan adjacent traces for each computed trace and describe the spatial and temporal relationships based on character such as phase, frequency, amplitude, etc. (Taner, 2001). Examples of these attributes are semblance, curvature, chaotic reflection, dip variance, dip of maximum similarity, and instantaneous lateral continuity. These attributes are referred to as "reflective attributes" which correspond to characteristics of interfaces between two beds. Each attribute's algorithm is computed differently. For example, semblance measures how similar the energy from a number of stacked traces compared to the total energy of all traces in that stack. This is computed mathematically by (Taner, 2002):

$$\boldsymbol{Semb}(\boldsymbol{t}) = \frac{\sum_{\tau=-N/2}^{\tau=N/2}\{\sum_{m=1}^{M} \boldsymbol{f}_m(\boldsymbol{t}+\boldsymbol{\tau})\}^2 - \sum_{\tau=-N/2}^{\tau=N/2}\sum_{m=1}^{M} \boldsymbol{f}_m^2(\boldsymbol{t}+\boldsymbol{\tau})}{\sum_{\tau=-N/2}^{\tau=N/2}\sum_{m=1}^{M} \boldsymbol{f}_m^2(\boldsymbol{t}+\boldsymbol{\tau})}$$

where fm(t) is the m^{th} trace of the gather and N is the window length.

Another effective attribute in distinguishing the leakage response is the curvature attribute. Curvature is a second derivative of surface-derived attribute. It is a measure of deviation at a certain point from a straight line (Roberts 2001). A plane with a constant dip, for example, has zero curvature value. When dip is variable, curvature is non-zero. To compute curvature from a grid of measurements, an approximation method such as the least-squares fitting is used. Chopra and Marfurt (2007) and Roberts (2001) show more details of using the approximation method to fit a quadratic surface in the form of

$$z(x,y) = ax^2 + cxy + by^2 + dx + ey + f$$

where a, b, c, d, e, and f are coefficients computed from the values of grid nodes and the distance between these nodes.

Based on this approximation, computations are made to derive different curvature values such as maximum, minimum, mean, Gaussian, most positive and most negative curvatures. The latter two always show the same polarity for geologic events such as faults, folds and fractures (Chopra and Markfurt, 2007). Most-positive and most-negative curvature were used to detect the gas leakage in this study. The most-postive curvature is calculated from the previous quadratic surface equation by

$$K_{pos} = (a + b) + \sqrt{(a - b)^2 + c^2}$$

and the most-negative curvature is calculated by

$$K_{neg} = (a + b) - \sqrt{(a - b)^2 + c^2}$$

RESULTS AND DISCUSSION

In the Te Kiri seismic volume, the presence of fault-related gas leakage was first observed on vertical sections. Figure 3 shows an example of a normal fault cutting through the Eocene reservoir sequences. Associated with this fault is a zone of disrupted seismic reflections showing the gas leakage characteristics previously described. The root of this leakage zone seems to have been originated beneath the Eocene reservoir level. The leakage zone resembles a cone-shape chaotic response which appears as a zone of vertical incoherence extending almost to the surface. This leakage zone appears to be relatively lower amplitude, whereas the top of the zone shows bright spots. These bright spots are high amplitudes caused by a strong drop in acoustic impedance. The observation of bright spots is often a direct indicator of the presence of gas.

The response of this leakage zone seems to be well-distinguished on seismic attributes. The effects of waves traveling through low velocity zones show as disruptions in coherency of the data. This translates to very low semblance values along the leakage zone. Disrupted signals also result in high values of curvature. This is probably due to changes in geometric local dips as a result of scattering within the leakage zone. The dip changes are evident on dip variance attributes.

It was observed that the gas presence generally fell within the extreme ends of certain attributes' spectrum. For example, the leakage zone was represented by the lowest semblance (Figure 4) and highest curvature values (Figure 5).

This observation is particularly useful when it comes to a quick-look interpretation for the distribution of possible leakage in the survey. When attribute values are analyzed, they can be filtered to show only the representative leakage response. The filtered values should be based on analysis of several sections at leakage zones from different locations. These values could also be shown on a horizontal slice to indicate the distribution of potential leakage in the survey (Figure 5). It is important to check the quality of the results since the displayed values depends on the interpreter's chosen filter. For example, if a poor filter is chosen for semblance attribute, it is possible to include values caused by low similarity across a non-leaking fault.

Since computations of different attributes follow different algorithms, it is possible that non-leakage-related response showing in one attribute is avoided by another. When multi-attributes are filtered and overlain on each other, a better estimate of leakage distribution is shown (Figure 6). The more values from different attributes are shown at a given location, the higher the chance of having a leakage-like response at that location.

Meldahl et al, (1998) and Aminzadeh et al (2001) describe a developed multi-attributes approach for pattern recognition though neural networks. The use of multi-

attributes has proven to be effective in detecting geologic features such as gas chimneys. This method require several picks for chimney and non-chimney samples. If interpreters have access to this neural network software, a better estimate is possible for the gas locations. If the software access is not available or minimum initial picks are desired, then the work described in this report might serve to be useful in the early stages of interpretation.

This study identified naturally occurring gas leakages using filtered attributes that distinguish the leakage response. The concepts behind this study can also be applied to detect leakages from non-naturally occurring gas in the subsurface. CO_2 leakage to shallow aquifers, for example, is a critical issue. Challenges and responsibilities are vast when dealing with cases where reservoirs are not confined or knowledge about seal integrity is lacking (Lawton, 2010). The concepts in this study can possibly serve to be valuable if utilized for seismic surveys before and after gas injections for monitoring purposes.

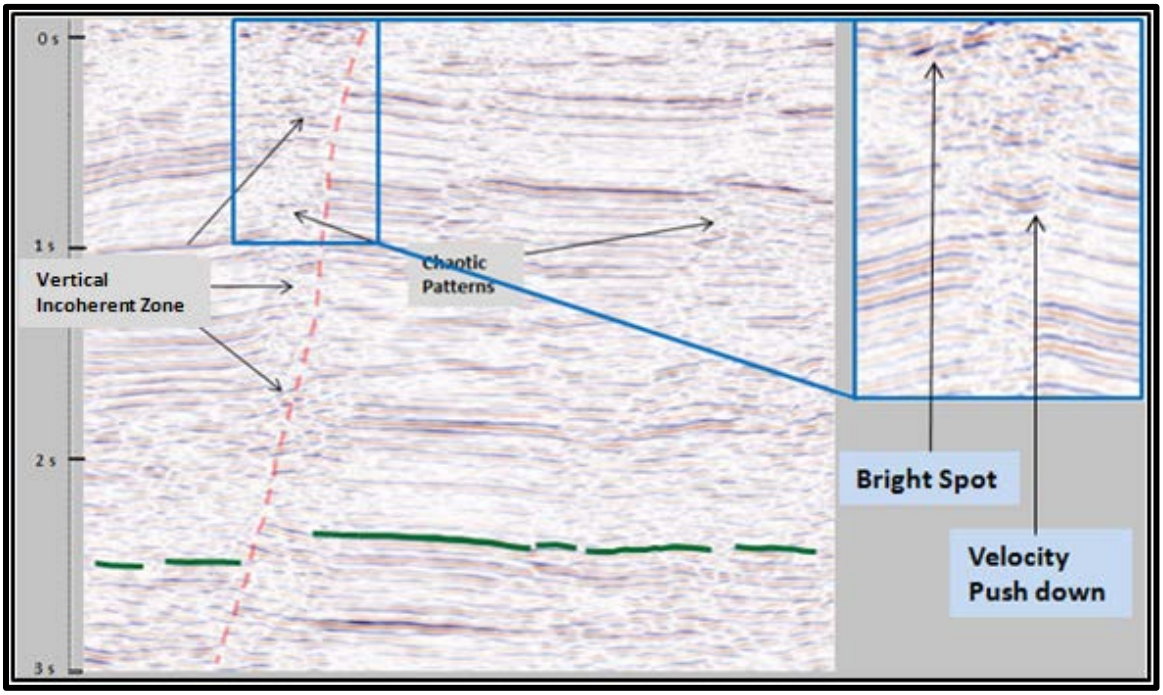

Figure 3: Effects of gas leakage on seismic amplitude section. Non-sealing fault is indicated in red. In green, top Eocene sandstone reservoir which had hydrocarbon shows from Te Kiri-1 well.

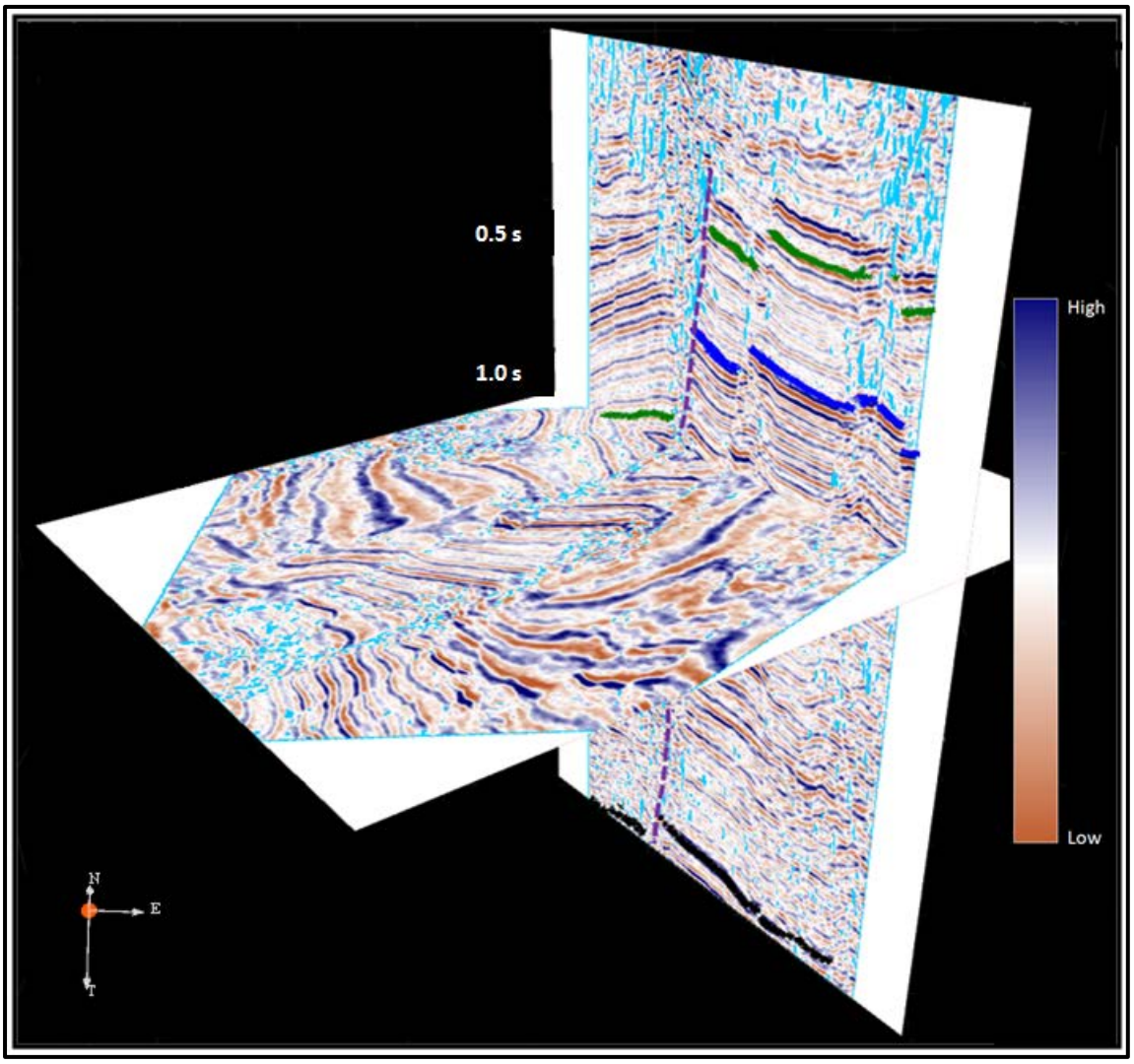

Figure 4: Distribution of low semblance (light blue) superimposed on amplitude sections. These values predict the location of leakage-like response. Higher semblance values were filtered (transparent). Leaking normal fault (purple) was interpreted to cut through the top of reservoir (black) and two other interpreted horizons (blue and green).

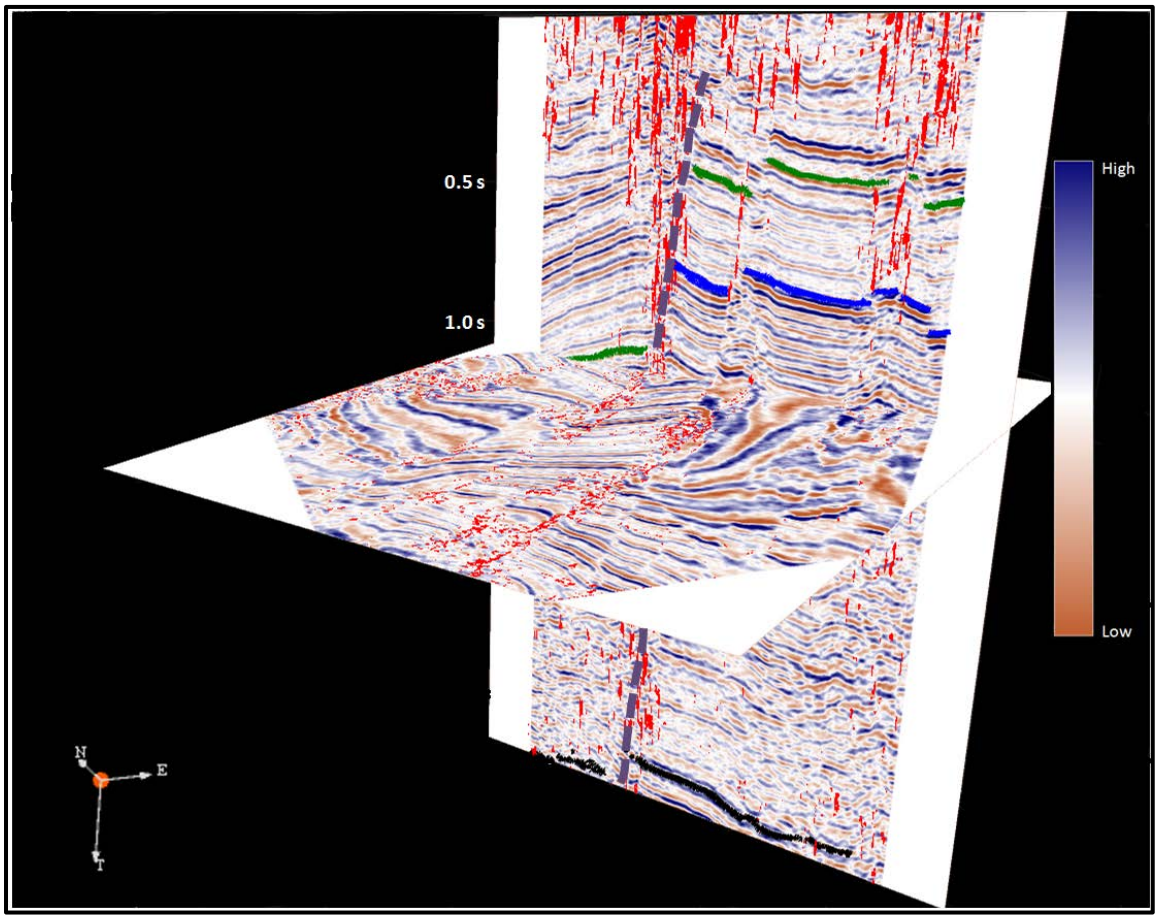

Figure 5: High values of most-positive curvature (red) overlaid on amplitude sections. These values predict the location of leakage-like response. Lower curvature values were filtered (transparent). Leaking normal fault (purple) was interpreted to cut through the top of reservoir (black) and two other interpreted horizons (blue and green).

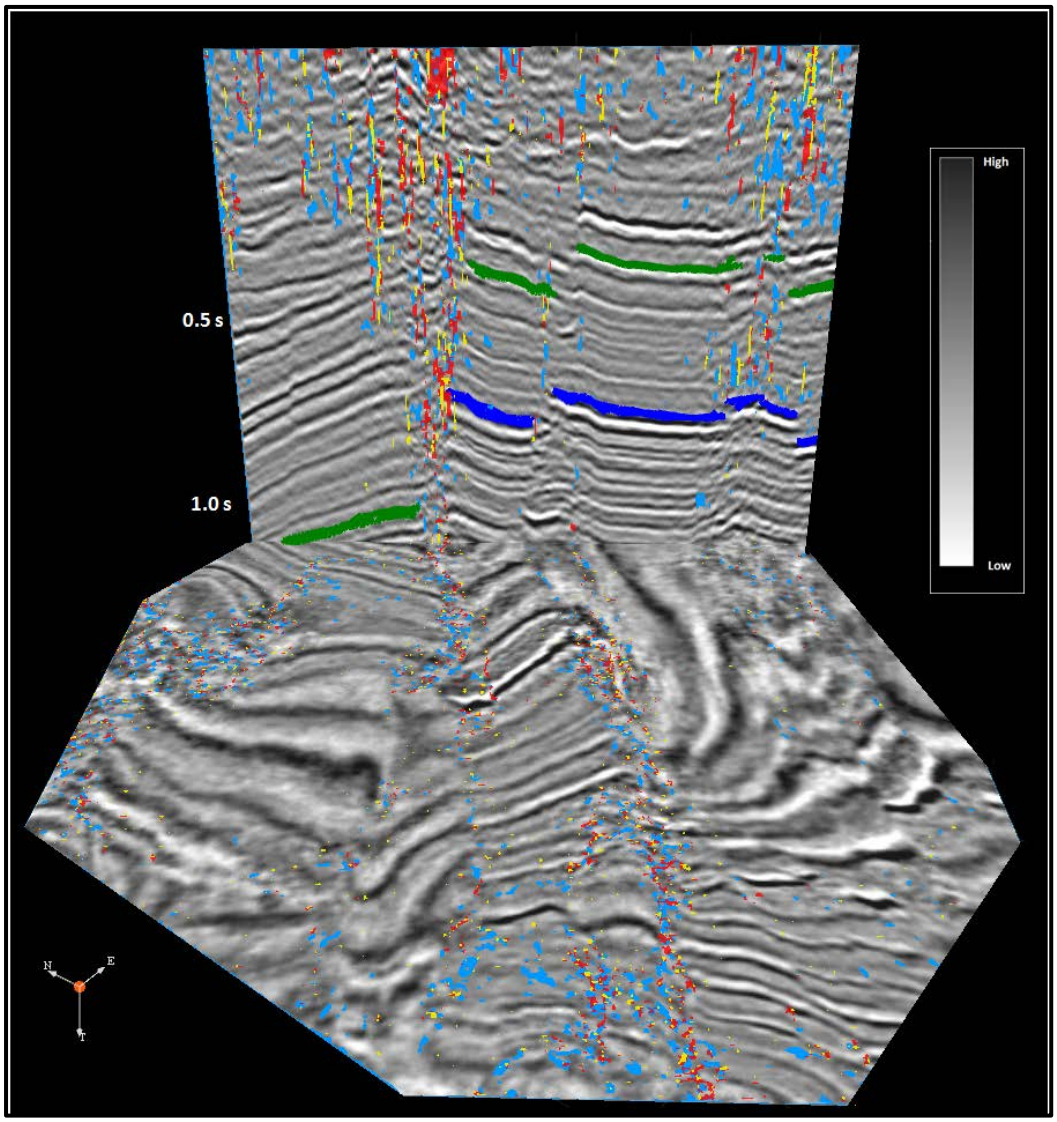

Figure 6: multi-attributes overlaid on vertical and horizontal amplitude sections to predict leakage locations. Filtered values are shown for semblance (light blue), most positive curvature (red) and most negative curvature (yellow). The more attributes shown within the same locality, the higher is the chance for gas presence.

CONCLUSIONS

Gas leakages are identified in Te Kiri 3D survey along normal faults. The interpretation of gas presence is supported by observations of amplitude anomalies and incoherent reflections within the leakage zone. The anomalies and signal incoherency are caused by scattering, attenuation, and reduction in P-wave velocity. Attributes such as semblance and curvature are helpful in detecting unique responses caused by gas presence. When filtered and combined together, these attributes can assist in delineating the gas-leakage distributions in the survey. The results from this work can serve to be useful in early stages of interpretation as well as a useful tool for monitoring gas injection and storage.

ACKNOWLEDGMENTS

We would like to thank Saudi Aramco and the CREWES Project for providing financial and technical support. Seismic data for this study was obtained from the Ministry of Economic Development of New Zealand. The software used for interpretations was Kingdom Suite.

REFERENCES:

Alshuhail, A., and Lawton, D. C., 2007, Time-lapse surface seismic monitoring of injected CO2 at the Penn West CO2-EOR site, Violet Grove, Alberta, CREWES Research Report, 19

Aminzadeh, F., Connolly, D., Heggland, R., Meldahl, P., de Groot, P., 2002. Geohazard detection and other applications of chimney cubes: The Leading Edge, 681–685

Anderson, A. L., and L. D. Hampton, 1980a, Acoustics of gas-bearing sediments: 1. Background: Journa of the Acoustical Society of America, 67, 1865–1889

Bjørkum, P. A., Walderhaug, O. and Nadeau, P. H., 1998, Physical constraints on hydrocarbon leakage and trapping revisited: EAGE Petroleum Geoscience, 4, 237-239

Chopra, S., Marfurt, K. J., 2007, Seismic attributes for prospect identification and reservoir characterization: SEG geophysical developments series, no. 11

Ilg, B. R. , Hemmings-Sykes, S., Nicol, A., Baur, J., Fohrmann, M., Funnell, R., and Milner, M., 2012, Normal faults and gas migration in an active plate boundary, southern Taranaki Basin, offshore, New Zealand: AAPG Bulletin, v. 96, No. 9, 1733-1756

King, P. R., and G. P. Thrasher, 1996, Cretaceous–Cenozoic geology and petroleum systems of the Taranaki Basin, New Zealand: Lower Hutt, Institute of Geological and Nuclear Sciences (New Zealand) monograph 13

Lawton, D., 2010, Carbon capture and storage: opportunities and challenges for geophysics: CSEG RECORDER, 7-10

Lawton, D. C., Bertram M. B., Margrave, G. F. and Gallant, E. V., Comparisons between data recorded by several 3-component coil geophones and a MEMS sensor at the Violet Grove monitor seismic survey: CREWES Research Report, 18

Løseth, H., M. Gading, and L. Wensaas, 2009, Hydrocarbon leakage interpreted on seismic data: Marine and Petroleum Geology, v. 26, no. 7, 1304–1319

Mavko, G., Mukerji, T., and Dvorkin, J., 2003, The Rock Physics Handbook, 51 p. Cambridge University Press, Cambridge, U.K.

Meldahl, P., R. Heggland, B. Bril, and P. de Groot, 2001, Identifying faults and gas chimneys using multiattributes and neural networks: Leading Edge, v. 20, no. 5, p. 474–482

MUIR, R. J., BRADSHAW, J. D., WEAVER, S. D., and LAIRD, M. G., 2000,The influence of basement structure on the evolution of the Taranaki Basin, New Zealand: Journal of the Geological Society of London, 157, Part 6:1179-1185

Roberts, A., 2001, Curvature attributes and their application to 3D interpreted horizons: First Break, 19, 85–99

Stewart, et al, 2003, Converted-wave seismic exploration: Applications: GEOPHYSICS, 68/1. (January-Febraury); 40-57

Taner, M. T. , 2001, Seismic Attributes: CSEG Recorder, 48-56

Taner, M. T., 2002, System for estimating the locations of shaley subsurface formations: U.S. Patent No. 6,487,502. 2

Todd Energy, 2006, Te Kiri 3D Seismic Interpretation Report; Ministry of Economic Development New Zealand Unpublished Report PR3595